Stem Cell Reports
Resource
OPEN ACCESS

Differentiation of Inflammation-Responsive Astrocytes from Glial Progenitors Generated from Human Induced Pluripotent Stem Cells

Renata Santos,[1,2,7] Krishna C. Vadodaria,[1,7] Baptiste N. Jaeger,[1,7] Arianna Mei,[1] Sabrina Lefcochilos-Fogelquist,[1] Ana P.D. Mendes,[1] Galina Erikson,[3] Maxim Shokhirev,[3] Lynne Randolph-Moore,[1] Callie Fredlender,[1] Sonia Dave,[1] Ruth Oefner,[1] Conor Fitzpatrick,[4] Monique Pena,[1] Jerika J. Barron,[1] Manching Ku,[3] Ahmet M. Denli,[1] Bilal E. Kerman,[1,8] Patrick Charnay,[2] John R. Kelsoe,[5,6] Maria C. Marchetto,[1] and Fred H. Gage[1,*]

[1]Laboratory of Genetics, The Salk Institute for Biological Studies, 10010 North Torrey Pines Road, La Jolla, CA 92037, USA
[2]Ecole Normale Supérieure, PSL Research University, CNRS, Inserm, Institut de Biologie de l'Ecole Normale Supérieure (IBENS), 46 rue d'Ulm, 75005 Paris, France
[3]The Razavi Newman Integrative Genomics and Bioinformatics Core Facility
[4]Flow Cytometry Core Facility
The Salk Institute for Biological Studies, 10010 North Torrey Pines Road, La Jolla, CA 92037, USA
[5]Department of Psychiatry, VA San Diego Healthcare System, La Jolla, CA 92151, USA
[6]Department of Psychiatry, University of California San Diego, La Jolla, CA 92093, USA
[7]Co-first author
[8]Present address: Research Center for Regenerative and Restorative Medicine (REMER), Istanbul Medipol University, Kavacık Mah. Ekinciler Cad. No.19 Beykoz, 34810 Istanbul, Turkey
*Correspondence: gage@salk.edu
http://dx.doi.org/10.1016/j.stemcr.2017.05.011

SUMMARY

Astrocyte dysfunction and neuroinflammation are detrimental features in multiple pathologies of the CNS. Therefore, the development of methods that produce functional human astrocytes represents an advance in the study of neurological diseases. Here we report an efficient method for inflammation-responsive astrocyte generation from induced pluripotent stem cells (iPSCs) and embryonic stem cells. This protocol uses an intermediate glial progenitor stage and generates functional astrocytes that show levels of glutamate uptake and calcium activation comparable with those observed in human primary astrocytes. Stimulation of stem cell-derived astrocytes with interleukin-1β or tumor necrosis factor α elicits a strong and rapid pro-inflammatory response. RNA-sequencing transcriptome profiling confirmed that similar gene expression changes occurred in iPSC-derived and primary astrocytes upon stimulation with interleukin-1β. This protocol represents an important tool for modeling in-a-dish neurological diseases with an inflammatory component, allowing for the investigation of the role of diseased astrocytes in neuronal degeneration.

INTRODUCTION

Astrocytes are a major component of the human CNS. The versatile and heterogeneous nature of astrocytes allows them to perform multiple essential functions during brain development and later in neuronal homeostasis and synaptic transmission. Astrocytes are essential for the establishment and plasticity of neural circuits since they participate in the formation of synapses, in the phagocytic removal of unwanted synapses, and in neurotransmitter recycling (Khakh and Sofroniew, 2015). Astrocytes are located close to blood vessels and participate in the formation of the blood-brain barrier and in the regulation of blood flow. They regulate extracellular ion concentrations and provide energy and substrates to neurons (Sofroniew and Vinters, 2010). In addition to these sustaining functions, astrocytes participate in the response to injury and disease by becoming reactive. Astrocyte reactivity is a graded and complex response that includes changes in morphology, gene expression, and inflammation (Anderson et al., 2014; Colombo and Farina, 2016; Pekny and Pekna, 2014; Sofroniew, 2009, 2015). Morphological changes range from hypertrophy and polarization toward the site of injury to the formation of glial scars. Genomic studies using two injury mouse models, ischemic stroke and neuroinflammation, revealed extensive modifications in the transcriptome profiles of reactive astrocytes with a common gene component and gene changes specific to each stimulus (Zamanian et al., 2012). As a result, the role of astrocyte dysfunction and neuroinflammation in multiple CNS pathologies is attracting attention (Pekny et al., 2015).

During embryonic development, radial glial cells generate progenitors that differentiate into neurons in the early embryonic phase and into glial cells in the late embryonic and postnatal periods. This switch from neurogenesis to gliogenesis involves epigenetic changes and Notch signaling (Fan, 2005; Morrison et al., 2000; Takizawa et al., 2001). Notch activates the JAK/STAT3 (Janus kinase/signal transducer and activator of transcription 3)

This is an open access article under the CC BY-NC-ND license (http://creativecommons.org/licenses/by-nc-nd/4.0/).

pathway, which promotes astrogliogenesis (Kamakura et al., 2004). In mice, astrocyte progenitors migrate radially from the germinal ventricular zone and occupy a stable territory throughout the life of the animal (Tsai et al., 2012). Thus, morphological and functional astrocyte diversity is determined during development by the regional patterning of the precursors (Hochstim et al., 2008; Tsai et al., 2012). Data obtained from in vitro culture astrocytes purified from human and rat brains showed that human astrocytes occupy an extended territory and display a superior total arborization length (Zhang et al., 2016). Indeed, significant differences exist between human and rodent astrocytes (Han et al., 2013; Oberheim et al., 2006, 2009; Zhang et al., 2016) that may be relevant for functional studies of astrocytes in the context of human neurological disorders.

Future studies of human astrocyte response to inflammation require reliable in vitro models. Human astrocytes can be cultured from fetal and adult biopsies; however, the availability of CNS human tissue is reduced and immunopanning is required to obtain pure astrocyte preparations (Zhang et al., 2016). The generation of astrocytes from induced pluripotent stem cells (iPSCs) has the advantage of obtaining access to astrocyte phenotypes and their effects on neuronal physiology from patients with neurodegenerative and neuropsychiatric diseases. However, the development of efficient protocols to generate astrocytes in a dish from stem cells is hindered by insufficient knowledge of astrocyte specification during development and in the adult CNS and by the lack of specific proteins expressed by astrocytes that can be used as markers (Molofsky et al., 2012). Recently, Zhang et al. (2016) identified human astrocyte-specific genes and differences in transcription between astrocyte precursors and mature astrocytes. Current available protocols focus on recapitulating the gliogenic switch observed during embryonic development (Chandrasekaran et al., 2016; Emdad et al., 2012; Krencik and Zhang, 2011; Roybon et al., 2013; Serio et al., 2013; Shaltouki et al., 2013; Tyzack et al., 2016). Human iPSCs (hiPSCs) or human embryonic stem cells (hESCs) are converted into neural progenitor cells (NPCs) and then patterned and switched to glial progenitor cells (GPCs) that eventually differentiate and mature into astrocytes. Recently, the conversion of mouse and human fibroblasts into astrocytes using small-molecule induction has been described (Tian et al., 2016). Despite the role that astrocytes play in neuroinflammation, few studies have reported the generation of pro-inflammatory astrocytes (Holmqvist et al., 2015; Roybon et al., 2013). In this study, we describe an efficient protocol to derive functional astrocytes from glial progenitors that show a rapid inflammatory response after stimulation with interleukin-1β (IL-1β) or tumor necrosis factor α (TNF-α).

RESULTS

Generation of Human Astrocytes from iPSCs and ESCs through Differentiation of Intermediate GPCs

Existing protocols for differentiation of astrocytes from human iPSCs or ESCs attempt to recapitulate embryonic development by first generating NPC intermediates before differentiating them into GPCs and finally into astrocytes (Chandrasekaran et al., 2016; Tyzack et al., 2016). Current methods are time consuming, and it is unclear whether the derived astrocytes are inflammation responsive; hence we sought to generate inflammation-responsive astrocytes in a short period of time. We devised a method to efficiently derive GPCs from PSCs, including iPSCs and ESCs, such that they can be propagated, expanded, and frozen as intermediates (Figure 1A). Free-floating embryoid bodies were prepared from three iPSC cell lines and the hESC-H1 cell line and cultured in Astrocyte medium (ScienCell) in the presence of Noggin for 2 weeks for neural induction by SMAD inhibition (Chambers et al., 2009). Platelet-derived growth factor (PDGF) was added for 3 weeks to induce the JAK/STAT pathway, which is necessary for astrogliosis and oligodendrogenesis (Bonni et al., 1997; Fan, 2005; Dell'Albani et al., 1998; He et al., 2005). The identity of the GPCs was confirmed by the near ubiquitous expression of Nestin and of A2B5 antigen, which is a cell surface ganglioside known to be expressed in astrocyte precursors (Figures 1B and 1C). In addition, the nuclear factor IA (NFIA) is highly expressed in GPC (Figures 1B and 1C). NFIA is a transcriptional factor downstream of Notch that is necessary for the initiation of gliogenesis (Deneen et al., 2006).

For the differentiation and maturation of astrocytes, a neuronal medium with leukemia inhibitory factor (LIF) and serum was used (Figure 1A). LIF also activates the JAK/STAT signaling pathway (He et al., 2005). After 4–6 weeks of differentiation from the GPCs, we found high expression of key astrocytic markers, such as CD44 antigen, S100β (S100 calcium-binding protein), and glial fibrillary acidic protein (GFAP), as for primary astrocytes (Figures 1B–1D). Although the expression of GFAP was almost ubiquitous, the fluorescence levels detected were faint, suggesting low expression, which was confirmed by western blotting (Figure 1D). Expression of the aldehyde dehydrogenase 1 family member L1 (ALDH1L1), an early marker of astrocyte maturation, was also detected in a large percentage of primary astrocytes and ESC/iPSC-derived astrocytes but in a lower percentage of the population compared with the other markers (Figures 1B and 1C). Maturing astrocytes are known to express EAAT1 and EAAT2 (excitatory amino acid transporter 1/2), which are Na^+-dependent glutamate/aspartate transporters. Using western blotting, we found that 4-week-old iPSC-derived astrocytes

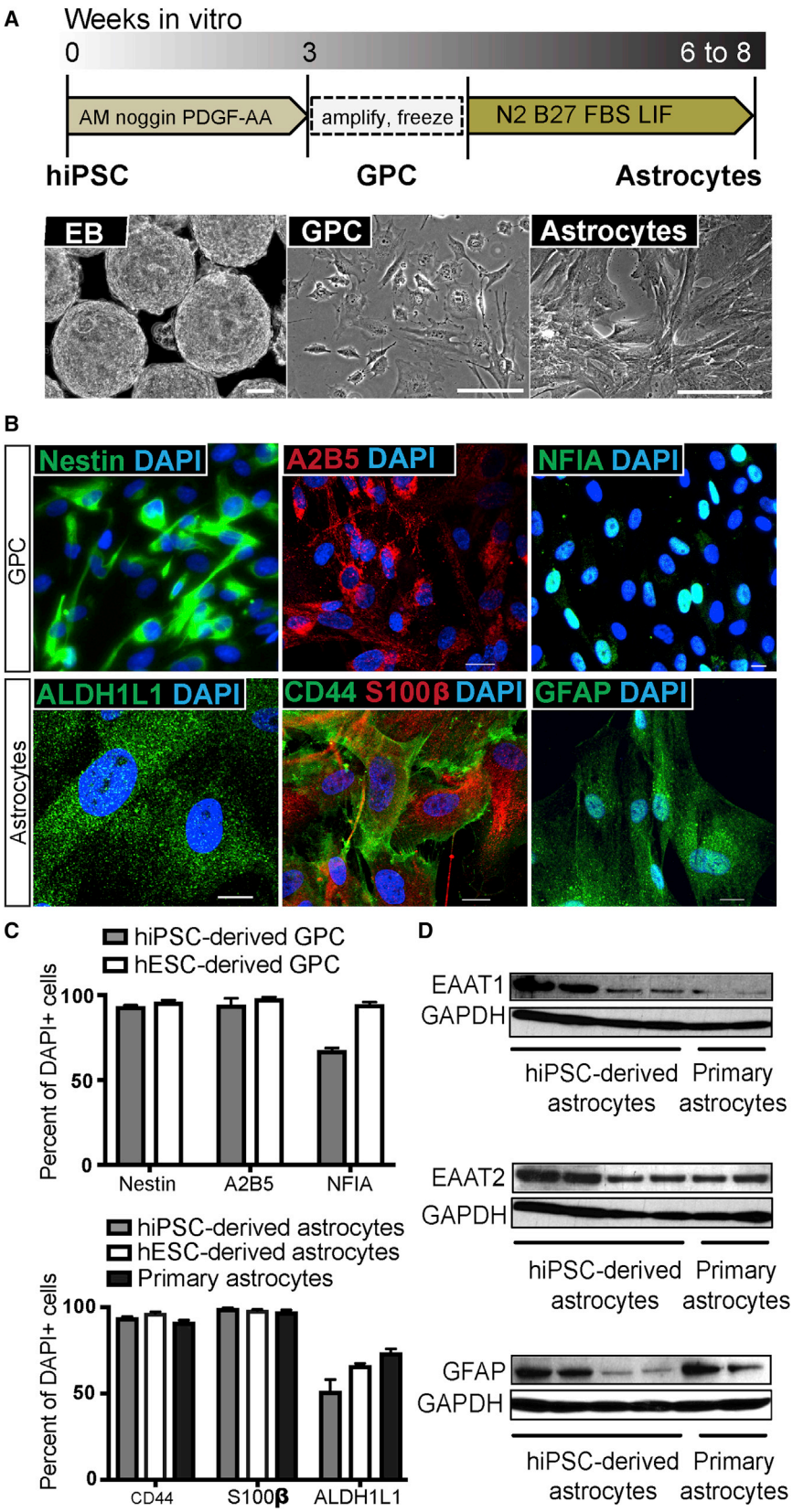


Figure 1. Differentiation of Astrocytes from Stem Cells via Glial Progenitor Cells

(A) Schematic representation of the experimental paradigm used for differentiation of human astrocytes over a total time of 6–8 weeks. Human iPSCs or ESCs were used to generate floating embryoid bodies (EB), followed by dissociated glial progenitor cells (GPC), and were differentiated to astrocytes in monolayers (shown are representative bright-field images for cells at each stage). Scale bars, 20 μm.

(B) Representative fluorescent images of immunostainings for ESC- and iPSC-derived GPCs expressing Nestin (green), A2B5 (red), or NFIA (green), and astrocytes (4-week differentiation post GPC; 6-week differentiation for GFAP) expressing ALDH1L1 (green), CD44 (green)/S100β (red), or GFAP (green). All cells were counterstained for DAPI (blue). Scale bars, 20 μm.

(C) Quantifications for percentage of cells, GPCs, or astrocytes, positive for the listed markers over DAPI. Results are expressed as means ± SEM, n = 3 experiments for iPSC-derived lines or n = 3 experiments for hESC-derived lines and primary astrocytes.

(D) Representative western blots showing expression of EAAT1, EAAT2, and GFAP (4-week differentiation post GPC) in iPSC-derived astrocytes or in cerebellar primary astrocytes. GAPDH was used as a total protein loading control.

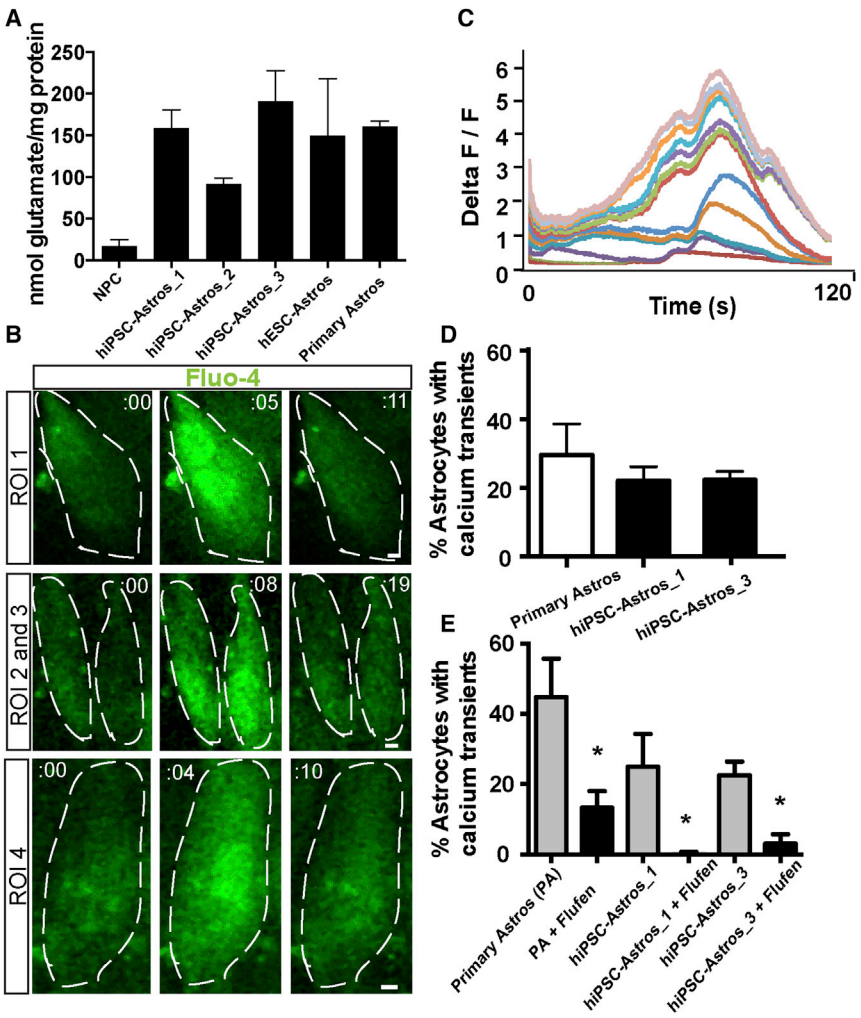


Figure 2. Differentiated Astrocytes from Human iPSCs and ESCs Are Functional

(A) Na^+-dependent [^{3}H]glutamate transport in 6-week-old astrocytes differentiated from iPSCs, ESCs, and human primary astrocytes is similar. Neural progenitor cells (NPC) were used as a negative control.

(B) Representative montages of Fluo-4 containing green astrocytes labeled as distinct regions of interest (ROI) at different time points (seconds). Scale bar, 20 μm.

(C) Twelve individual traces of calcium transients (various colors) of astrocytes represented as change in fluorescence/minimum fluorescence ($\Delta F/F_{min}$) over time (seconds).

(D) Graph shows percentage of the population of astrocytes per video displaying calcium transients in a period of 120 s.

(E) Graph depicts percentage of astrocytes displaying calcium transients in different treatment groups (with or without flufenamic acid).

Data are presented as mean ± SEM, n = 3 experiments. Statistical analysis by Mann-Whitney test; *p < 0.05 (primary = 0.032; iPSC1 = 0.012; iPSC2 = 0.004).

expressed both EAAT1 and EAAT2 protein (Figure 1D). Interestingly, we found higher protein levels of EAAT2 compared with EAAT1 in both iPSC-derived and primary astrocytes. These results agree with developmental observations that EAAT1 is expressed during development and EAAT2 is expressed in the mature brain and accounts for 90% of glutamate transport in astrocytes (Kim et al., 2011). Remarkably, neuron differentiation from the GPCs was never observed in astrocyte cultures immunostained with anti-MAP2 antibody (Figure S1).

In summary, using the current protocol from hiPSCs, we were able to efficiently generate GPCs and astrocytes, as determined by the expression of key astrocytic markers in vitro.

iPSC/ESC-Derived Astrocytes Actively Take Up Glutamate and Display Calcium Transients

We next examined whether the generated astrocytes were functionally mature. A hallmark of astrocyte function is glutamate uptake from the extracellular space (Robinson and Jackson, 2016). Na^+-dependent glutamate uptake corresponds to the activity of EAAT1/2 transporters and can be measured directly using a radioactive assay. We observed that primary astrocytes and iPSC/ESC-derived 6-week-old astrocytes were able to take up glutamate at comparable levels, suggesting the functional activity of EAAT1/2 in the astrocytes in vitro (Figure 2A). This result is in agreement with the expression of glutamate transporters (Figure 1D).

Astrocytes are known to exhibit waves of calcium transients in a characteristic manner (Bazargani and Attwell, 2016; Rusakov, 2015; Shigetomi et al., 2016; Stout et al., 2002). Using Fluo-4, a calcium-responsive dye, we examined calcium activity in the generated astrocytes. We found that astrocytes displayed slow calcium transients over a period of 2 min (Figures 2B and 2C; Movies S1, S2, and S3), which are distinct from fast neuronal calcium transients. Quantification of the percentage of astrocytes

displaying transients showed that approximately 25% of the iPSC-derived astrocytes were active over a span of 2 min, similar to what was observed for primary human cerebellar astrocytes (Figure 2D). Astrocytes are capable of widespread intercellular communication, as observed by propagated waves of calcium transients. These waves are thought to be laterally propagated at least in part via gap junctions. Therefore, we next examined whether 50 μM flufenamic acid (flufen), a gap junction inhibitor, regulated calcium transients in iPSC-derived astrocytes. iPSC-derived astrocytes and primary astrocytes showed more than a 50% reduction in the percentage of cells displaying calcium transients (Figure 2E and Movie S4), suggesting that functional gap junctions enabled the propagation of calcium waves in vitro.

Together, our data suggest that the iPSC-derived astrocytes not only expressed markers of maturing astrocytes but also functionally took up glutamate, displayed typical calcium transients, and showed functional gap junction-regulated calcium activity in vitro.

Differentiated Astrocytes Respond to Pro-inflammatory Stimuli

Astrocytes are immunocompetent cells that participate in neuroinflammation by secreting cytokines and chemokines, which may have protective or detrimental consequences for neuronal survival (Colombo and Farina, 2016). Thus far, attempts to generate immunocompetent human astrocytes have met with limited success. Two studies using long protocols (between 13 and 18 weeks) for differentiation of ventral midbrain and spinal cord astrocytes reported the production of inflammatory cytokines and chemokines by ELISA or protein arrays after stimulation with IL-1β or TNF-α for 7 days (Holmqvist et al., 2015; Roybon et al., 2013). However, using these assays it is difficult to quantify the proportion of the cellular population that becomes effectively reactive, which is an important piece of information for functional assays.

Given the relevance of neuroinflammation in the context of neurological diseases, we sought to examine whether the astrocytes generated by our protocol were immunocompetent. To test whether the astrocytes that we generated produced cytokines upon pro-inflammatory stimuli, we utilized a flow cytometry-based approach classically applied to immune cells (Jung et al., 1993; Picker et al., 1995). In this assay, astrocytes were stimulated in the presence of monensin and brefeldin A, which disrupt the Golgi-mediated protein transport, leading to an intracellular accumulation of produced cytokines (Figure 3A). Five hours post stimulation, astrocytes were fixed and permeabilized to enable the detection of intracellular IL-6 and IL-8 cytokines using directly conjugated antibodies. Percentages of IL-6- and IL-8-producing astrocytes were quantified by flow cytometry (Figure 3B). In contrast to the ELISA assay, which measures the total amount of cytokines produced within a population of cells, this method allows the quantification of the number of cytokine-producing cells within a population. We observed high cell survival rates (>90%) following treatment with protein transport inhibitors in both the non-stimulated and stimulated conditions (Figure 3C) and no changes in cellular morphology (Figure 3D). The production of IL-6 and IL-8 in all non-stimulated samples was low (Figure 3E), indicating that the inhibition of protein transport by monensin and brefeldin A did not promote the inflammatory response observed in the IL-1β- or TNF-α-treated groups. To further validate our assay, we pre-incubated ESC- and iPSC-derived astrocytes with an IL-1β receptor antagonist (IL-1RA) for 1 hr before adding IL-1β (Figure S2). Blocking IL-1 receptor in the presence of IL-1β drastically reduced the percentages of IL-8- and IL-6-producing astrocytes, demonstrating that the pro-inflammatory response measured in astrocytes was specific to the IL-1β stimulation.

Using this flow cytometry-based approach, we next assessed the percentage of reactive primary astrocytes and 4-week differentiated iPSC/ESC-derived astrocytes following IL-1β or TNF-α pro-inflammatory treatment (Figures 3F and 3G). The response to IL-1β stimulation was stronger than to TNF-α stimulation in all astrocytic cell lines. Also, upon inflammatory stimulation a larger percentage of astrocytes produced IL-8 (stem cell-derived IL-1β-stimulated astrocytes: 71.4% ± 3.73%; TNF-α-stimulated: 37.0% ± 2.24%) than IL-6 (stem cell-derived IL-1β-stimulated astrocytes: 40.9% ± 3.71%; TNF-α-stimulated: 16.0% ± 2.70%). Despite inter-donor variability, iPSC-derived astrocytes were found to be robustly reactive at levels comparable with primary and ESC-derived astrocytes. These results suggest that, similar to primary astrocytes, iPSC-derived human astrocytes are immunocompetent as they not only responded to inflammatory stimuli but could also further sustain inflammation by producing pro-inflammatory cytokines themselves.

Transcriptomic Analysis of IL-1β-Stimulated Astrocytes

To examine the transcriptomic inflammatory signature in response to pro-inflammatory cytokines, we performed RNA sequencing (RNA-seq) analysis of IL-1β-stimulated iPSC-derived astrocytes in the absence of monensin and brefeldin A. Unsupervised hierarchical clustering of IL-1β-stimulated astrocytes derived from three iPSC lines, in duplicates, revealed that stimulated and non-stimulated astrocytes clustered separately (Figure 4A). Similarly, stimulated and non-stimulated iPSC-derived astrocytes separated out distinctly in principal component analysis, suggesting that the transcriptional signature of stimulated astrocytes

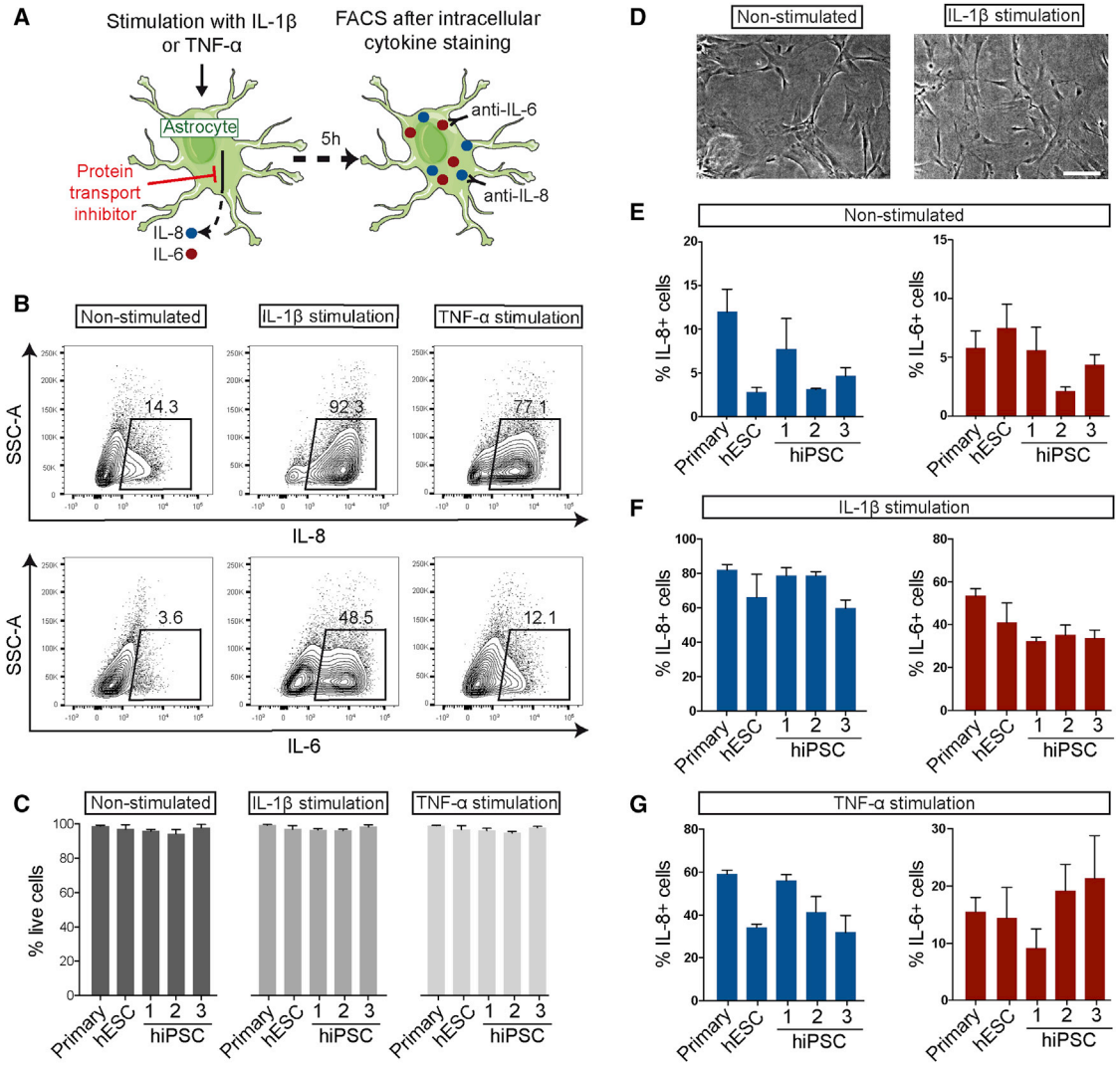


Figure 3. Pro-inflammatory Cytokine Production in Response to Inflammatory Stimulation Is Comparable between iPSC-Derived Astrocytes and Primary Astrocytes

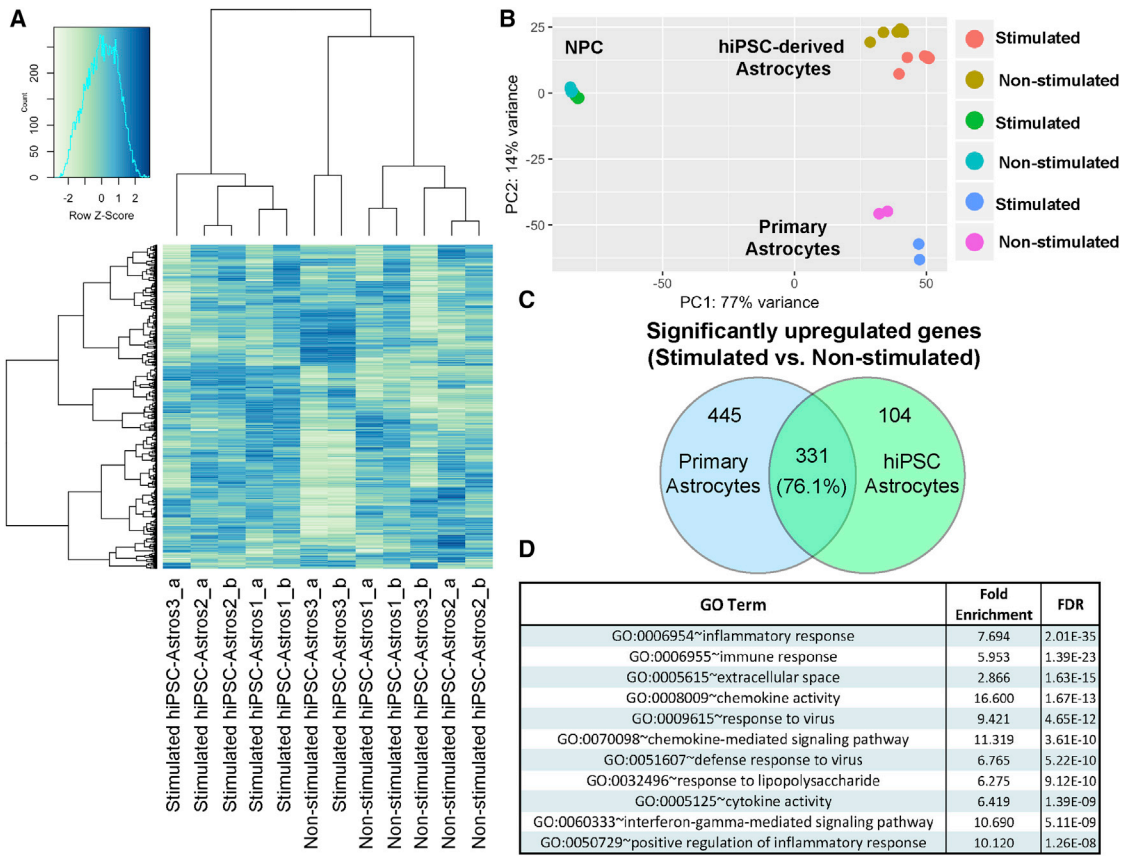
(A) Experimental paradigm used to assess pro-inflammatory cytokine production at a single-cell level in astrocyte cultures. Primary, ESC-derived, or iPSC-derived astrocytes were stimulated with IL-1β (10 ng/mL) or TNF-α (50 ng/mL), or left in medium with vehicle. Protein transport inhibitors were added to the cultures to block the release of produced cytokines. Five hours later, cells were stained intracellularly with antibodies against IL-8 and IL-6. The percentage of cytokine-producing cells was then analyzed by flow cytometry.

(B) Representative FACS plots showing percentages of IL-8-positive (top) and IL-6-positive (bottom) primary cerebellar astrocytes 5 hr after stimulation with media + vehicle (Non-stimulated), IL-1β, or TNF-α, in the presence of protein transport inhibitors.

(C) Bar graphs showing the percentages of live astrocytes (negative for the viability dye Zombie UV), 5 hr after incubation with medium + vehicle (Non-stimulated), IL-1β, or TNF-α, in the presence of protein transport inhibitors (mean ± SD, n = 3 experiments).

(D) Representative bright-field images of iPSC-derived astrocytes 5 hr after incubation with (left) medium + vehicle (Non-stimulated) or (right) IL-1β, in the presence of protein transport inhibitors. Scale bar, 20 μm.

(E–G) Histograms showing the percentages of IL-8-positive (blue) and IL-6-positive (red) astrocytes of indicated primary or stem cell-derived cultures, 5 hr after incubation with (E) medium + vehicle (Non-stimulated), (F) IL-1β, or (G) TNF-α, in the presence of protein transport inhibitors (mean ± SD, n = 3 experiments). Background activation obtained in the non-stimulated condition was subtracted from stimulated conditions (mean ± SEM, n = 3 experiments).



GO Term	Fold Enrichment	FDR
GO:0006954~inflammatory response	7.694	2.01E-35
GO:0006955~immune response	5.953	1.39E-23
GO:0005615~extracellular space	2.866	1.63E-15
GO:0008009~chemokine activity	16.600	1.67E-13
GO:0009615~response to virus	9.421	4.65E-12
GO:0070098~chemokine-mediated signaling pathway	11.319	3.61E-10
GO:0051607~defense response to virus	6.765	5.22E-10
GO:0032496~response to lipopolysaccharide	6.275	9.12E-10
GO:0005125~cytokine activity	6.419	1.39E-09
GO:0060333~interferon-gamma-mediated signaling pathway	10.690	5.11E-09
GO:0050729~positive regulation of inflammatory response	10.120	1.26E-08

Figure 4. Transcriptomic Analysis of IL-1β-Stimulated Astrocytes

Whole transcriptomic analysis was performed on stimulated and non-stimulated primary astrocytes, iPSC-derived astrocytes, and neural progenitor cells (NPC).

(A) Unsupervised hierarchical clustering of the whole transcriptome of non-stimulated and IL-1β-stimulated iPSC-derived astrocytes and of iPSC-derived astrocytes. Replicates are referred as "a" and "b."

(B) Principal component (PC) analysis of IL-1β-stimulated astrocytes shows distinct clustering of activated and non-activated iPSC-derived astrocytes, iPSC-derived NPCs, and primary astrocytes.

(C) Venn diagram depicts overlapping set of significantly upregulated genes following IL-1β stimulation between primary astrocytes and iPSC-derived astrocytes, with percentage of overlapping genes shown.

(D) Table shows gene ontology (GO) analysis for all genes significantly upregulated in stimulated versus non-stimulated iPSC-derived astrocytes. Listed are GO terms, fold enrichment of genes in each category, and false discovery rate (FDR) corrected p values for each GO term.

represents an acutely distinct state (Figure 4B). To further confirm the specificity of the inflammatory signature of iPSC-derived astrocytes, we compared the whole transcriptome of stimulated and non-stimulated samples with NPCs derived from the same iPSC lines and with primary astrocytes. The NPCs were used as negative controls since they did not show a significant production of pro-inflammatory cytokines (IL-6 and IL-8) upon IL-1β stimulation (Figure S3). To understand the nature of the genes upregulated following IL-1β stimulation, we compared the sets of genes upregulated in primary astrocytes with iPSC-derived astrocytes (Figure 4C). A total of 776 and 435 genes were significantly upregulated in stimulated primary astrocytes and iPSC-derived astrocytes, respectively. We found that 331 genes were common between these lists (Table S1), which accounted for more than 76% of genes upregulated in iPSC-derived astrocytes and 42% of genes upregulated in primary astrocytes, showing a substantial overlap in the pathways upregulated in primary and iPSC-derived astrocytes following IL-1β stimulation (Figure 4C). To further characterize the upregulated pathways in an unbiased manner, we performed gene ontology (GO) analysis of all significantly upregulated genes in iPSC-derived astrocytes. We filtered GO categories on the basis of highest significance corrected for false discovery rate and found a 2- to 16-fold enrichment for inflammation-related GO terms

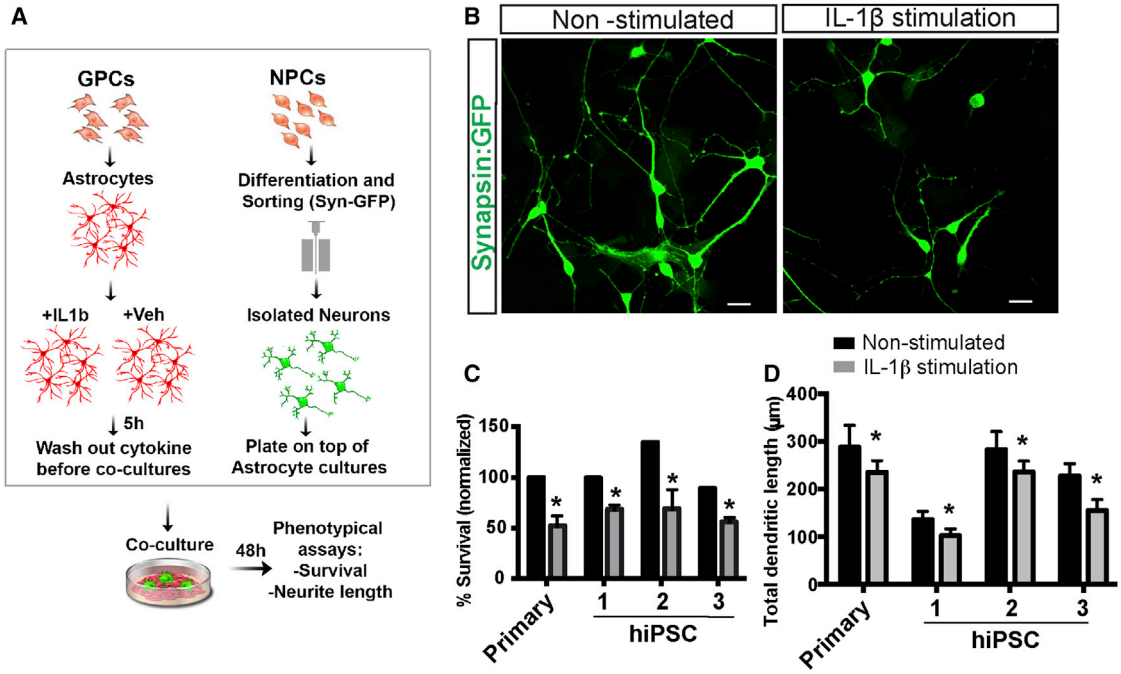


Figure 5. Astrocytes Differentiated from iPSCs Behave in a Similar Fashion to Primary Astrocytes in Co-cultures with Neurons

(A) Experimental paradigm of the co-culture experiment. FACS-sorted 4-week-old neurons were plated on top of astrocytes differentiated for 4 weeks from GPCs stimulated or not with IL-1β for 5 hr. Neuronal survival and morphological maturation (neurite length) was assayed following 48 hr of co-culture.

(B) Representative confocal images of immunostainings of synapsin-GFP-expressing neurons after co-culture with astrocytes. Scale bars, 20 μm.

(C) iPSC-derived astrocytes can support neuronal survival. Treatment of astrocytes with pro-inflammatory cytokine IL-1β affects neuronal survival similarly in co-cultures with primary or iPSC-derived astrocytes.

(D) Maturation of neurons measured by dendritic length is similar in primary and iPSC-derived astrocytes but is affected by IL-1β pre-treatment on astrocytes.

Statistical analysis on independent triplicates: two-way ANOVA following outlier removal, *$p < 0.01$ ($p = 0.006$; $n = 3$ for C and $n = 15$ neurons per line from independent triplicates for D). Results are expressed as means ± SEM.

such as inflammatory response, immune response, chemokine activity, and cytokine activity (Figure 4D).

Inflammatory Stimulation of iPSC-Derived Astrocytes Affects Neuron Viability and Morphology

To study the functional consequences of pro-inflammatory astrocytes on neurons, we used an in vitro co-culture assay in which synapsin-positive neurons were isolated by fluorescence-activated cell sorting (FACS) and plated on top of 4-week-old astrocytes that had been previously treated with vehicle or stimulated with IL-1β for 24 hr (Figure 5A). Sorted neurons were co-cultured with astrocytes for 48 hr in the absence of cytokines. Following fixation, neuronal survival and neurite outgrowth were assayed for co-cultures with iPSC/ESC-derived and primary astrocytes. We observed that a significantly lower percentage of neurons co-cultured with IL-1β pre-treated astrocytes compared with vehicle pre-treated astrocytes (Figure 5B). Similarly, we observed a drastic reduction in the dendritic length of neurons co-cultured with astrocytes pre-treated with IL-1β (Figures 5C and 5D). These data suggest that stimulation of inflammatory response in iPSC-derived astrocytes directly affects neuronal viability and morphology. The results of these experiments indicate that stimulated astrocytes have a sustained and direct impact on neuronal maturation and survival even after a washout of the pro-inflammatory cytokines, suggesting that the protocol described here can be used for modeling neurological diseases with an inflammatory component.

DISCUSSION

Along with microglia and other non-neural cells, astrocytes participate in the inflammatory response of the CNS to injury and disease by producing cytokines, chemokines, pro-oxidant molecules, and signaling factors (DiSabato et al., 2016; Sofroniew, 2015). Astrocytes also play an

important role in maintaining brain function homeostasis, and their dysfunction can trigger progression of neurodegenerative diseases (Chandrasekaran et al., 2016). Much of our current knowledge on astrocyte biology comes from the study of rodents. Recently it was shown that human astrocytes are intrinsically more complex than mouse astrocytes, and astrocytes express unique genes and respond differently to extracellular glutamate (Han et al., 2013; Oberheim et al., 2006, 2009; Zhang et al., 2016). Importantly, drugs that showed promising results in animal models have failed in human trials (Cavanaugh, 2014; Cummings et al., 2014; Rothstein, 2003; Waldmeier et al., 2006), possibly due to the different properties of human astrocytes. Therefore, the development of applicable and relevant human models for studying neurological disease mechanisms and testing drugs has become necessary. Here we report an efficient method for differentiating inflammation-responsive astrocytes from human iPSCs and ESCs.

A major breakthrough in the study of astrocytes was the description of a procedure to purify and culture astrocytes from neonatal rodent brains using serum-containing media (McCarthy and de Vellis, 1980). This protocol was used and modified for decades to culture not only rodent cells but also human astrocytes from fetal postmortem tissue (Ennas et al., 1992; Lee et al., 1993). Recently, new methods of astrocyte purification using immunopanning combined with serum-free culture have been described for adult rodent and human brains (Foo et al., 2011; Zhang et al., 2016). These methods are attractive because the selected astrocytes are functional and are expected to be more similar to their in vivo equivalents. However, these are invasive techniques; for example, the temporal lobe cortex tissue used by Zhang et al. (2016) was excised during surgery to expose the epileptic hippocampi, and the broad application of this technique to the study of human neurological disorders remains challenging. In addition, most neuroinflammatory, neurodegenerative, and psychiatric conditions are multigenic and poorly described genetically. Thus, cellular models that rely on the differentiation of astrocytes from iPSCs or other non-brain cell types are still the most accessible methods for in vitro disease modeling and can potentially allow for new discoveries. Indeed, astrocyte dysfunction was found in Costello and Down syndromes using iPSC-derived astrocytes uncovering new drug targets (Chen et al., 2014; Krencik et al., 2015).

Inflammation is one of the main features of neurodegenerative diseases (Campbell, 2004). Having methods available that generate human astrocytes that are responsive to inflammation allows for the modeling of this component of the disease using patients' cells. Previous studies reported the generation of reactive astrocytes after a 7-day treatment with IL-1β or TNF-α (Holmqvist et al., 2015; Roybon et al., 2013), but, as the authors used the ELISA assay or protein arrays to quantify chemokine and cytokine production, it is difficult to assess what proportion of the cellular population became effectively reactive. In our hands, classical protocols using iPSC-derived NPCs (Chandrasekaran et al., 2016; Tyzack et al., 2016) did not generate astrocytes responsive to pro-inflammatory stimuli using the FACS-based assay described in this study. Here we report a method for differentiating astrocytes using intermediate GPCs that were generated in a serum-containing medium that is reminiscent of the McCarthy-de Vellis astrocyte culture protocol (McCarthy and de Vellis, 1980). Because astrocytes contact blood vessels in vivo, it is possible that the serum contains unknown signals necessary for the differentiation of astrocytes responsive to inflammatory stimuli in culture.

The protocol presented here represents a robust tool for modeling neurological diseases with an inflammatory component, for example Parkinson's disease and Alzheimer's disease. It allows for investigating the role of diseased astrocytes in neurodegenerative disease and the possibility of screening new anti-inflammatory drugs. In addition, this protocol can also be used to explore the cell-autonomous role of astrocytes and inflammation in other disorders including certain psychiatric disorders.

EXPERIMENTAL PROCEDURES

Differentiation of Astrocytes from Human iPSCs and ESCs

The human iPSC lines used in this study were Sendai-reprogrammed from fibroblasts and correspond to control cell lines (NM1–4; here named as hiPSC1–4 for simplicity), as described by Mertens et al. (2015). All subjects provided written informed consent and all procedures were approved by local human subjects committees. iPSC and hESC H1 (WiCell Research Institute) lines were cultured on Matrigel-coated plates in mTeSR1 medium (STEMCELL Technologies). Embryoid bodies were prepared from confluent stem cell cultures by mechanical dissociation with 1 mg/mL collagenase IV (Invitrogen), plated onto low-adherence plates in mTeSR1 medium with 10 μM ROCK inhibitor (Axxora), and incubated overnight with agitation. For differentiation of GPC in the embryoid bodies, Astrocyte medium (AM, ScienCell) supplemented with 500 ng/mL Noggin (Peprotech) and 10 ng/mL PDGFAA (R&D Systems) was used for 14 days and then, for 1 more week, supplemented only with PDGFAA. The embryoid bodies were dissociated with papain (Papain dissociation system, Worthington), and the GPC were cultured and expanded in 10 μg/mL poly-L-ornithine (Sigma)/1 μg/mL laminin (Invitrogen)-coated plates in AM supplemented with 20 ng/mL fibroblast growth factor 2 (Joint Protein Central) and 20 ng/mL epidermal growth factor (Peprotech). Astrocytes were differentiated from low-confluent GPC cultures in DMEM/F12 Glutamax (Thermo Fisher Scientific) supplemented with N2 and B27 (both from Thermo Fisher Scientific) and 10% fetal bovine serum (FBS, Omega

Scientific). Human LIF (10 ng/mL, Alomone Labs) was added for the first 2 weeks of differentiation. After 2 weeks of differentiation, the cells were transferred to non-coated plates. The human fetal primary astrocytes from cerebellum were purchased from ScienCell and cultured in AM. The NPC cell lines used in this study were derived from the same iPSC lines and cultured using previously described protocols (Mertens et al., 2015; Yu et al., 2014).

Immunocytochemistry

The cells plated on plastic slides were fixed with 4% paraformaldehyde solution for 15 min at room temperature. Antigen blocking and cell permeabilization were done using 10% horse serum and 0.1% Triton X-100 in PBS for 1 hr at room temperature. Primary antibodies were incubated in 10% horse serum overnight at 4°C, and the secondary antibodies (1:250, Jackson Laboratories) were incubated in the same solution for 1 hr at room temperature. The cells were counterstained with DAPI for detection of nuclei. The following primary antibodies were used: mouse anti-Nestin (1:500; EMD Millipore), rabbit anti-S100β (1:1,000; Dako), mouse anti-GFAP monoclonal (1:250; EMD Millipore), rat anti-CD44 (1:100; BD Pharmingen), rabbit anti-NFIA (1:250; Novus Bio), mouse anti-ALDH1L1 (1:100; EMD Millipore), mouse immunoglobulin M (IgM) anti-A2B5 (1:50; EMD Millipore). For A2B5 detection in live unfixed cells, the cells were incubated with anti-A2B5 antibody in DMEM/F12 Glutamax medium at 37°C for 40 min. After washing in warm PBS, fixation and secondary antibody application were performed as described above.

Flow Cytometry Assay for Cytokine Stimulation

Astrocytes differentiated for 4 weeks and primary human astrocytes were incubated for 5 hr with protein transport inhibitors (1:1,000; BD GolgiPlug, BD GolgiStop; BD Biosciences) and 10 ng/mL recombinant human IL-1β (R&D) or with 50 ng/mL recombinant human TNF-α (R&D) or PBS (vehicle) for the non-stimulated sample. For IL-1β receptor antagonist (IL-1RA) experiments, astrocytes were pre-incubated with carrier-free recombinant human IL-1RA (Biolegend) at 10 ng/mL for 1 hr prior to 5 hr of stimulation with 10 ng/mL IL-1β, 10 ng/mL IL-1RA, and protein transport inhibitors. After stimulation, the cells were dissociated for 1 min at room temperature in a mixture of 1:1 Accutase (STEMCELL)/papain (Papain dissociation system, Worthington), and washed and stained with the viability dye Zombie UV fixable kit (Biolegend). Cells were then fixed and permeabilized using the BD Cytofix/Cytoperm and BD Perm/Wash (BD Biosciences). The IL-6 and IL-8 cytokines were detected after incubation for 20 min at 4°C in BD Perm/Wash containing PerCP conjugated anti-IL-8 (BH0814) and APC conjugated anti-IL-6 (MQ213A5) antibodies (Biolegend). Data from labeled samples were acquired using a BD CantoII cytometer (BD Biosciences) followed by analysis using FlowJo software (TreeStar). Stainings with rat IgG1-APC (Biolegend, RTK2071) and mouse IgG2b-PercP (Biolegend, MPC-11) were used for negative gating controls for anti-IL-6 and anti-IL-8, respectively. Negative gates were defined using unstimulated conditions.

Calcium Imaging

5- to 7-week-old astrocyte cultures were loaded with the calcium-sensitive dye Fluo-4. Fluo-4 was prepared according the manufacturer's instructions from an imaging kit (Life Technologies) and directly added to culture medium. Astrocyte cultures were incubated with 1 μM Fluo-4 for 15 min at 37°C. Cells were washed with medium once and imaged immediately. Live fluorescent imaging was performed using a Zeiss spinning-disk confocal microscope, using a standard fluorescein isothiocyanate filter, and images were taken every 131 ms with the 20× objective for 120 s. Five areas with visibly spread astrocytes were selected for imaging for each line, and experiments were repeated three times. For quantification of change in intensity over time, astrocytes were outlined as regions of interest (ROI) and analyzed using ImageJ software. For each ROI, change in fluorescence intensity over time (ΔF) was plotted. Values were normalized to the minimum fluorescence (F_{min}) value for each individual ROI and representative traces are presented as $\Delta F/F_{min}$ over time. The percentage of cells activated was counted manually by an observer blinded to the groups, counting how many ROIs in each video displayed transients (examples of traces shown in Figure 2) compared with the total number of visible ROIs.

RNA-Seq Library Construction and Sequencing

RNA-seq analysis was performed in non-stimulated astrocytes and 4-week-old astrocytes stimulated for 5 hr with 10 ng/mL IL-1β (without protein transport inhibitors) and NPCs derived from the same iPSC lines. Details of the method are provided in Supplemental Experimental Procedures.

Astrocyte-Neuron Co-cultures

For the co-culture experiments, GPC were plated at 1×10^5 cells per well on 4-well chamber slides and further differentiated for 4 weeks into astrocytes (see scheme in Figure 4A). The astrocytes were then activated with cytokine IL-1β on day 28 of differentiation for 5 hr and washed with PBS to remove the residual cytokine before the addition of sorted neurons. For the neuronal co-cultures, 4-week-old neurons (cell line WT126, iPSC [Marchetto et al., 2010]) infected with a lentiviral vector expressing GFP under the control of synapsin promoter (Lenti-Syn:GFP) were sorted by FACS. Sorted neurons were plated on top of the astrocytes (20,000 neurons per well of a 4-well chamber slide) in neuronal induction medium (DMEM/F12 with N2, B27, 2% FBS, and laminin) without the addition of IL-1β. The neurons were co-cultured with the astrocytes for the following 48 hr. The co-cultures were then fixed with 4% paraformaldehyde and immunocytochemistry performed with GFP (1:500 chicken anti-GFP; Aves Labs) for quantification of the percentage of survival and the neurite length. Neuronal survival was calculated by counting the number of GFP-positive neurons 48 hr after co-culture and comparing this with the total number of cells plated. In brief, we counted the number of cells that attached in the well and divided it by the number of GFP neurons plated following the cell sorting. We performed the experiment in triplicate. For the neurite outgrowth assays, images were processed using ZEN Imaging software (Carl Zeiss Microscopy). Neurolucida (MBF Bioscience 11) was used to reconstruct individual GFP-labeled neurons after co-culture, and to perform subsequent morphological analyses along with Mirosoft Excel. A total of 15–20 neurons per astrocyte line for each treatment (IL-1β or vehicle) were analyzed.

ACCESSION NUMBERS

Data can be downloaded from the GEO database (GEO: GSE97619).

SUPPLEMENTAL INFORMATION

Supplemental Information includes Supplemental Experimental Procedures, three figures, one table, and four movies and can be found with this article online at http://dx.doi.org/10.1016/j.stemcr.2017.05.011.

AUTHOR CONTRIBUTIONS

R.S., K.C.V., B.N.J., and M.C.M. designed the study, performed experiments, analyzed the data, and wrote the manuscript. A.M., S.L.-F., S.D., C. Fredlender, A.M.D., and B.E.K. performed experiments and analyzed the data. A.P.D.M., L.R.-M., J.J.B., R.O., M.P., and C. Fitzpatrick performed experiments. G.E., M.S., and K.C.V. performed RNA-seq data analysis. M.K. helped perform RNA-seq experiments. P.C. and J.R.K. contributed with materials. F.H.G. contributed to the design of the study and interpretation of the results and edited the manuscript.

ACKNOWLEDGMENTS

For the production of the iPSCs, the authors would like to acknowledge financial support from Janssen Pharmaceuticals. This work was supported by the Paul G. Allen Family Foundation, Bob and Mary Jane Engman, The JPB Foundation, The Leona M. and Harry B. Helmsley Charitable Trust grant #2012-PG-MED002, Annette C. Merle-Smith, R01 MH095741 (F.H.G.), U19MH106434 (F.H.G.), and The G. Harold & Leila Y. Mathers Foundation. This work was supported by the Flow Cytometry Core Facility of the Salk Institute with funding from NIH-NCI CCSG: P30 014195; the Next Generation Sequencing Core Facility of the Salk Institute with funding from NIH-NCI CCSG: P30 014195; the Chapman Foundation and the Helmsley Charitable Trust and by The Razavi Newman Integrative Genomics and Bioinformatics Core Facility of the Salk Institute with funding from NIH-NCI CCSG: P30 014195. This research was also supported by the Swiss-NSF outgoing PD fellowship (K.C.V.), Lynn and Edward Streim fellowship (K.C.V.), EMBO long-term fellowship (B.N.J.), the Bettencourt Schueller Foundation (B.N.J.), and the Philippe Foundation (B.N.J.). The authors would like to thank M.L. Gage for editorial comments.

Received: January 5, 2017
Revised: May 9, 2017
Accepted: May 10, 2017
Published: June 6, 2017

REFERENCES

Anderson, M.A., Ao, Y., and Sofroniew, M.V. (2014). Heterogeneity of reactive astrocytes. Neurosci. Lett. *565*, 23–29.

Bazargani, N., and Attwell, D. (2016). Astrocyte calcium signaling: the third wave. Nat. Neurosci. *19*, 182–189.

Bonni, A., Sun, Y., Nadal-Vicens, M., Bhatt, A., Frank, D.A., Rozovsky, I., Stahl, N., Yancopoulos, G.D., and Greenberg, M.E. (1997). Regulation of gliogenesis in the central nervous system by the JAK-STAT signaling pathway. Science *278*, 477–483.

Campbell, A. (2004). Inflammation, neurodegenerative diseases, and environmental exposures. Ann. N.Y. Acad. Sci. *1035*, 117–132.

Cavanaugh, S.E. (2014). Animal models of Alzheimer disease: historical pitfalls and a path forward. ALTEX *31*, 279–302.

Chambers, S.M., Fasano, C.A., Papapetrou, E.P., Tomishima, M., Sadelain, M., and Studer, L. (2009). Highly efficient neural conversion of human ES and iPS cells by dual inhibition of SMAD signaling. Nat. Biotechnol. *27*, 275–280.

Chandrasekaran, A., Avci, H.X., Leist, M., Kobolák, J., and Dinnyés, A. (2016). Astrocyte differentiation of human pluripotent stem cells: new tools for neurological disorder research. Front. Cell. Neurosci. *10*, 215.

Chen, C., Jiang, P., Xue, H., Peterson, S.E., Tran, H.T., McCann, A.E., Parast, M.M., Li, S., Pleasure, D.E., Laurent, L.C., et al. (2014). Role of astroglia in Down's syndrome revealed by patient-derived human-induced pluripotent stem cells. Nat. Commun. *5*, 1–18.

Colombo, E., and Farina, C. (2016). Astrocytes: key regulators of neuroinflammation. Trends Immunol. *37*, 608–620.

Cummings, J.L., Morstorf, T., and Zhong, K. (2014). Alzheimer's disease drug-development pipeline: few candidates, frequent failures. Alzheimers Res. Ther. *6*, 37.

Dell'Albani, P., Kahn, M.A., Cole, R., Condorelli, D.F., Giuffrida Stella, A.M., and de Vellis, J. (1998). Oligodendroglial survival factors, PDGF-AA and CNTF, activate similar JAK/STAT signaling pathways. J. Neurosci. Res. *54*, 191–205.

Deneen, B., Ho, R., Lukaszewicz, A., Hochstim, C.J., Gronostajski, R.M., and Anderson, D.J. (2006). The transcription factor NFIA controls the onset of gliogenesis in the developing spinal cord. Neuron *52*, 953–968.

DiSabato, D.J., Quan, N., and Godbout, J.P. (2016). Neuroinflammation: the devil is in the details. J. Neurochem. *139*, 136–153.

Emdad, L., D'Souza, S.L., Kothari, H.P., Qadeer, Z.A., and Germano, I.M. (2012). Efficient differentiation of human embryonic and induced pluripotent stem cells into functional Astrocytes. Stem Cells Dev. *21*, 404–410.

Ennas, M.G., Cocchia, D., Silvetti, E., Sogos, V., Riva, A., Torelli, S., and Gremo, F. (1992). Immunocompetent cell markers in human fetal astrocytes and neurons in culture. J. Neurosci. Res. *32*, 424–436.

Fan, G. (2005). DNA methylation controls the timing of astrogliogenesis through regulation of JAK-STAT signaling. Development *132*, 3345–3356.

Foo, L.C., Allen, N.J., Bushong, E.A., Ventura, P.B., Chung, W.S., Zhou, L., Cahoy, J.D., Daneman, R., Zong, H., Ellisman, M.H., and Barres, B.A. (2011). Development of a method for the purification and culture of rodent astrocytes. Neuron *71*, 799–811.

Han, X., Chen, M., Wang, F., Windrem, M., Wang, S., Shanz, S., Xu, Q., Oberheim, N.A., Bekar, L., Betstadt, S., et al. (2013). Forebrain engraftment by human glial progenitor cells enhances synaptic plasticity and learning in adult mice. Stem Cell *12*, 342–353.

He, F., Ge, W., Martinowich, K., Becker-Catania, S., Coskun, V., Zhu, W., Wu, H., Castro, D., Guillemot, F., Fan, G., et al. (2005). A positive autoregulatory loop of Jak-STAT signaling controls the onset of astrogliogenesis. Nat. Neurosci. *8*, 616–625.

Hochstim, C., Deneen, B., Lukaszewicz, A., Zhou, Q., and Anderson, D.J. (2008). Identification of positionally distinct astrocyte subtypes whose identities are specified by a homeodomain code. Cell *133*, 510–522.

Holmqvist, S., Brouwer, M., Djelloul, M., Diaz, A.G., Devine, M.J., Hammarberg, A., Fog, K., Kunath, T., and Roybon, L. (2015). Generation of pluripotent stem cell reporter lines for the isolation of and reporting on astrocytes generated from ventral midbrain and ventral spinal cord neural progenitors. Stem Cell Res. *15*, 203–220.

Jung, T., Schauer, U., Heusser, C., Neumann, C., and Rieger, C. (1993). Detection of intracellular cytokines by flow cytometry. J. Immunol. Methods *159*, 197–207.

Kamakura, S., Oishi, K., Yoshimatsu, T., Nakafuku, M., Masuyama, N., and Gotoh, Y. (2004). Hes binding to STAT3 mediates crosstalk between Notch and JAK-STAT signalling. Nat. Cell Biol. *6*, 547–554.

Khakh, B.S., and Sofroniew, M.V. (2015). Diversity of astrocyte functions and phenotypes in neural circuits. Nat. Neurosci. *18*, 942–952.

Kim, K., Lee, S.G., Kegelman, T.P., Su, Z.Z., Das, S.K., Dash, R., Dasgupta, S., Barral, P.M., Hedvat, M., Diaz, P., et al. (2011). Role of excitatory amino acid transporter-2 (EAAT2) and glutamate in neurodegeneration: opportunities for developing novel therapeutics. J. Cell. Physiol. *226*, 2484–2493.

Krencik, R., and Zhang, S.C. (2011). Directed differentiation of functional astroglial subtypes from human pluripotent stem cells. Nat. Protoc. *6*, 1710–1717.

Krencik, R., Hokanson, K.C., Narayan, A.R., Dvornik, J., Rooney, G.E., Rauen, K.A., Weiss, L.A., Rowitch, D.H., and Ullian, E.M. (2015). Dysregulation of astrocyte extracellular signaling in Costello syndrome. Sci. Transl. Med. *7*, 286ra66.

Lee, S.C., Liu, W., Dickson, D.W., Brosnan, C.F., and Berman, J.W. (1993). Cytokine production by human fetal microglia and astrocytes. Differential induction by lipopolysaccharide and IL-1β. J. Immunol. *150*, 2659–2667.

Marchetto, M.C.N., Carromeu, C., Acab, A., Yu, D., Yeo, G.W., Mu, Y., Chen, G., Gage, F.H., and Muotri, A.R. (2010). A model for neural development and treatment of Rett syndrome using human induced pluripotent stem cells. Cell *143*, 527–539.

McCarthy, K.D., and de Vellis, J. (1980). Preparation of separate astroglial and oligodendroglial cell cultures from rat cerebral tissue. J. Cell Biol. *85*, 890–902.

Mertens, J., Wang, Q.W., Kim, Y., Yu, D.X., Pham, S., Yang, B., Zheng, Y., Diffenderfer, K.E., Zhang, J., Soltani, S., et al. (2015). Differential responses to lithium in hyperexcitable neurons from patients with bipolar disorder. Nature *527*, 95–99.

Molofsky, A.V., Krenick, R., Ullian, E., Tsai, H.H., Deneen, B., Richardson, W.D., Barres, B.A., and Rowitch, D.H. (2012). Astrocytes and disease: a neurodevelopmental perspective. Genes Dev. *26*, 891–907.

Morrison, S.J., Perez, S.E., Qiao, Z., Verdi, J.M., Hicks, C., Weinmaster, G., and Anderson, D.J. (2000). Transient Notch activation initiates an irreversible switch from neurogenesis to gliogenesis by neural crest stem cells. Cell *101*, 499–510.

Oberheim, N.A., Wang, X., Goldman, S., and Nedergaard, M. (2006). Astrocytic complexity distinguishes the human brain. Trends Neurosci. *29*, 547–553.

Oberheim, N.A., Takano, T., Han, X., He, W., Lin, J.H.C., Wang, F., Xu, Q., Wyatt, J.D., Pilcher, W., Ojemann, J.G., et al. (2009). Uniquely hominid features of adult human astrocytes. J. Neurosci. *29*, 3276–3287.

Pekny, M., and Pekna, M. (2014). Astrocyte reactivity and reactive astrogliosis: costs and benefits. Physiol. Rev. *94*, 1077–1098.

Pekny, M., Pekna, M., Messing, A., Steinhäuser, C., Lee, J.M., Parpura, V., Hol, E.M., Sofroniew, M.V., and Verkhratsky, A. (2015). Astrocytes: a central element in neurological diseases. Acta Neuropathol. *131*, 323–345.

Picker, L.J., Singh, M.K., Zdraveski, Z., Treer, J.R., Waldrop, S.L., Bergstresser, P.R., and Maino, V.C. (1995). Direct demonstration of cytokine synthesis heterogeneity among human memory/effector T cells by flow cytometry. Blood *86*, 1408–1419.

Robinson, M.B., and Jackson, J.G. (2016). Astroglial glutamate transporters coordinate excitatory signaling and brain energetics. Neurochem. Int. *98*, 56–71.

Rothstein, J.D. (2003). Of mice and men: reconciling preclinical ALS mouse studies and human clinical trials. Ann. Neurol. *53*, 423–426.

Roybon, L., Lamas, N.J., Garcia-Diaz, A., Yang, E.J., Sattler, R., Jackson-Lewis, V., Kim, Y.A., Kachel, C.A., Rothstein, J.D., Przedborski, S., et al. (2013). Human stem cell-derived spinal cord astrocytes with defined mature or reactive phenotypes. Cell Rep. *4*, 1035–1048.

Rusakov, D.A. (2015). Disentangling calcium-driven astrocyte physiology. Nat. Rev. Neurosci. *16*, 226–233.

Serio, A., Bilican, B., Barmada, S.J., Ando, D.M., Zhao, C., Siller, R., Burr, K., Haghi, G., Story, D., Nishimura, A.L., et al. (2013). Astrocyte pathology and the absence of non-cell autonomy in an induced pluripotent stem cell model of TDP-43 proteinopathy. Proc. Natl. Acad. Sci. USA *110*, 4697–4702.

Shaltouki, A., Peng, J., Liu, Q., Rao, M.S., and Zeng, X. (2013). Efficient generation of astrocytes from human pluripotent stem cells in defined conditions. Stem Cells *31*, 941–952.

Shigetomi, E., Patel, S., and Khakh, B.S. (2016). Probing the complexities of astrocyte calcium signaling. Trends Cell Biol. *26*, 300–312.

Sofroniew, M.V. (2009). Molecular dissection of reactive astrogliosis and glial scar formation. Trends Neurosci. *32*, 638–647.

Sofroniew, M.V. (2015). Astrocyte barriers to neurotoxic inflammation. Nat. Rev. Neurosci. *16*, 249–263.

Sofroniew, M.V., and Vinters, H.V. (2010). Astrocytes: biology and pathology. Acta Neuropathol. *119*, 7–35.

Stout, C.E., Costantin, J.L., Naus, C.C.G., and Charles, A.C. (2002). Intercellular calcium signaling in astrocytes via ATP release through connexin hemichannels. J. Biol. Chem. *277*, 10482–10488.

Takizawa, T., Nakashima, K., Namihira, M., Ochiai, W., Uemura, A., Yanagisawa, M., Fujita, N., Nakao, M., and Taga, T. (2001). DNA methylation is a critical cell-intrinsic determinant of astrocyte differentiation in the fetal brain. Dev. Cell *1*, 749–758.

Tian, E., Sun, G., Sun, G., Chao, J., Ye, P., Warden, C., Riggs, A.D., and Shi, Y. (2016). Small-molecule-based lineage reprogramming creates functional astrocytes. Cell Rep. *16*, 781–792.

Tsai, H.H., Li, H., Fuentealba, L.C., Molofsky, A.V., Taveira-Marques, R., Zhuang, H., Tenney, A., Murnen, A.T., Fancy, S.P.J., Merkle, F., et al. (2012). Regional astrocyte allocation regulates CNS synaptogenesis and repair. Science *337*, 358–362.

Tyzack, G., Lakatos, A., and Patani, R. (2016). Human stem cell-derived astrocytes: specification and relevance for neurological disorders. Curr. Stem Cell Rep. *2*, 236–247.

Waldmeier, P., Bozyczko-Coyne, D., Williams, M., and Vaught, J.L. (2006). Recent clinical failures in Parkinson's disease with apoptosis inhibitors underline the need for a paradigm shift in drug discovery for neurodegenerative diseases. Biochem. Pharmacol. *72*, 1197–1206.

Yu, D.X., Di Giorgio, F.P., Yao, J., Marchetto, M.C., Brennand, K., Wright, R., Mei, A., McHenry, L., Lisuk, D., Grasmick, J.M., et al. (2014). Modeling hippocampal neurogenesis using human pluripotent stem cells. Stem Cell Reports *2*, 295–310.

Zamanian, J.L., Xu, L., Foo, L.C., Nouri, N., Zhou, L., Giffard, R.G., and Barres, B.A. (2012). Genomic analysis of reactive astrogliosis. J. Neurosci. *32*, 6391–6410.

Zhang, Y., Sloan, S.A., Clarke, L.E., Caneda, C., Plaza, C.A., Blumenthal, P.D., Vogel, H., Steinberg, G.K., Edwards, M.S.B., Li, G., et al. (2016). Purification and characterization of progenitor and mature human astrocytes reveals transcriptional and functional differences with mouse. Neuron *89*, 37–53.

Stem Cell Reports, Volume *8*

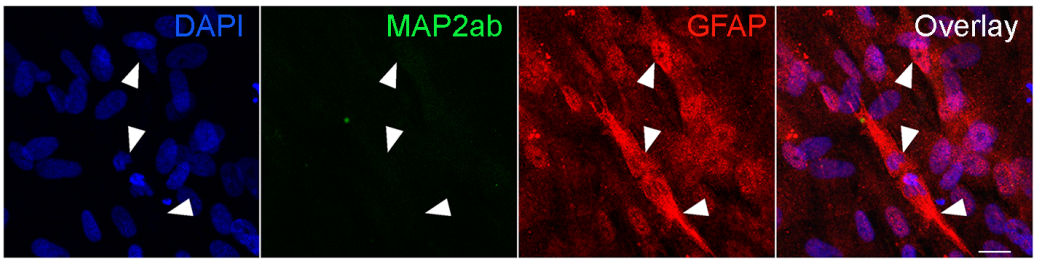
Supplemental Information

Differentiation of Inflammation-Responsive Astrocytes from Glial Progenitors Generated from Human Induced Pluripotent Stem Cells

Renata Santos, Krishna C. Vadodaria, Baptiste N. Jaeger, Arianna Mei, Sabrina Lefcochilos-Fogelquist, Ana P.D. Mendes, Galina Erikson, Maxim Shokhirev, Lynne Randolph-Moore, Callie Fredlender, Sonia Dave, Ruth Oefner, Conor Fitzpatrick, Monique Pena, Jerika J. Barron, Manching Ku, Ahmet M. Denli, Bilal E. Kerman, Patrick Charnay, John R. Kelsoe, Maria C. Marchetto, and Fred H. Gage

SUPPLEMENTAL FIGURES

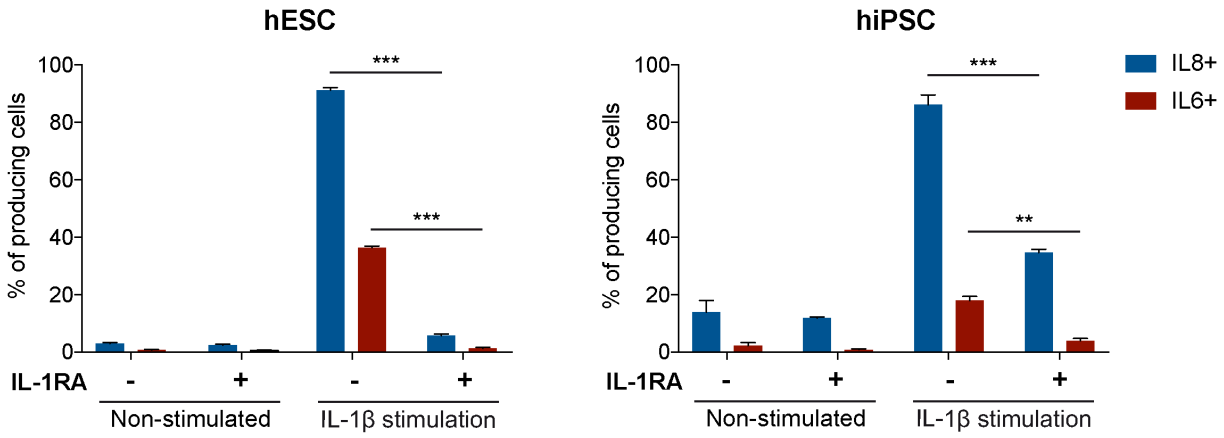
Supplemental Figure S1



Supplemental Figure S1.

GPC differentiate into astrocytes but not neurons. Shown are representative fluorescence images of immunostainings of MAP2ab (green) and GFAP (red) of astrocytic cultures differentiated 6 weeks post-GPC that were counterstained for DAPI (blue). The arrowheads point to GFAP-positive cells. Scale bar: 20 μm. Related to Figure 1.

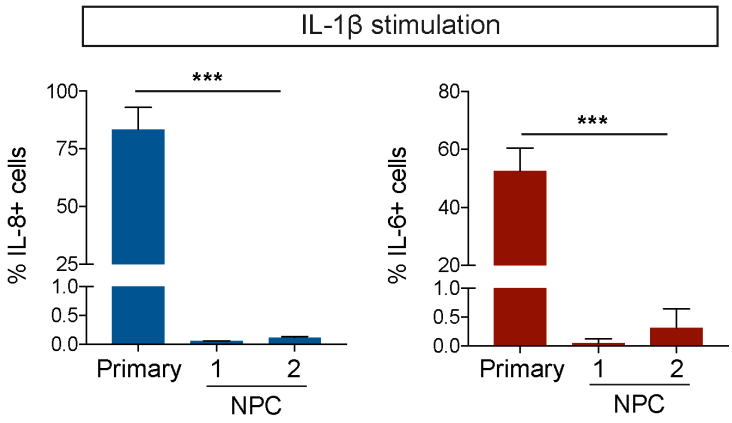
Supplemental Figure S2



Supplemental Figure S2.

Pro-inflammatory cytokine production is specific to IL-1β stimulation. ESC-derived and 5-week old iPSC-derived astrocytes (hiPSC_1) were pre-incubated in the absence (-) or presence of (+) IL-1β receptor antagonist (IL-1RA) for 1 h prior to 5 h incubation in media + vehicle (non-stimulated) or IL-1β, in the presence of protein transport inhibitors. Statistical analysis performed on independent triplicates- T-test *** $p < 0.001$, ** $p < 0.01$ (mean ± SD, n=3). Related to Figure 3.

Supplemental Figure S3



Supplemental Figure S3. **Neural progenitor cells do not respond to inflammatory stimulation.** Histograms showing the percentages of IL-8- (blue) and IL-6- (red) positive NPC derived from 2 iPSC lines, 5 h after incubation with IL-1β in the presence of protein transport inhibitors. Background activation obtained in the non-stimulated condition was subtracted from stimulated conditions (mean ± SD, n=3-9, T-test *** $p < 0.001$). Statistical analysis performed on independent triplicates. Related to Figure 4.

SUPPLEMENTAL VIDEOS

Video S1. Video showing calcium transients for hiPSC_1-derived astrocytes stained with fluo-4. Related to Figure 2.

Video S2. Video showing calcium transients for hiPSC_3-derived astrocytes stained with fluo-4. Related to Figure 2.

Video S3. Video showing calcium transients for cerebellar primary astrocytes stained with fluo-4. Related to Figure 2.

Video S4. Video showing calcium transients for hiPSC_1-derived astrocytes stained with fluo-4 and treated with 50 µM flufenamic acid. Related to Figure 2.

SUPPLEMENTAL EXPERIMENTAL PROCEDURES

Western Blotting

For Western blotting, cells were scraped from the dishes in RIPA buffer (Thermo Scientific) containing protease and phosphatase inhibitors (Thermo Scientific) and incubated for 5 min on ice. Lysates were clarified by centrifugation (14,000 x*g* for 15 min at 4°C) and Western immunoblotting was performed following standard procedures using the iBlot gel and transfer system (Life Technologies). Primary antibodies for mouse anti-EAAT1 (1:1,000; Santa Cruz), mouse anti-EAAT2 (1:1,000; Santa Cruz), rabbit anti-GFAP polyclonal (1:5,000; ThermoFisher Scientific), and mouse anti-GAPDH (1:5,000; Fitzgerald Industries International) were incubated sequentially (overnight at 4°C). Anti-mouse (1:5,000) horseradish peroxidase-coupled secondary antibodies were added (1 h at room temperature) and detected sequentially using ECL luminescence solution (Millipore) as per the manufacturer's instructions.

Glutamate Uptake

Glutamate uptake assay was performed according to Gupta et al. (2011). Astrocytes differentiated for 6 weeks were washed in warm Na^+-containing Krebs buffer (120 mM NaCl, 25 mM $NaHCO_3$, 5 mM KCl, 2 mM $CaCl_2$, 1 mM KH_2PO_4, 1 mM $MgSO_4$, 10% glucose) and then incubated in the same buffer containing 50 µM glutamate and 1 µCi ^{3}H-glutamic acid (47.5 Ci/nmol; PerkinElmer). The same procedure was performed with Na^+-free Krebs buffer (120 mM choline-Cl, 25 mM Tris-HCl pH 7.4, 5 mM KCl, 2 mM $CaCl_2$, 1 mM KH_2PO_4, 1 mM $MgSO_4$, 10% glucose). The cells were lysed in 0.1 N NaOH and the radioactivity was measured using a LS6500 (Beckman) scintillation counter. The Na^+-dependent glutamate uptake was calculated by subtracting the counts in Na^+-free buffer to the counts in Na^+-containing buffer.

RNA-seq Library Construction and Sequencing

Non-stimulated and 5-h 10 ng/ml IL-1β-stimulated 4-week-old astrocytes (without protein transport inhibitors) were collected in RNABee solution (Tel-test, Inc) and total RNA was extracted using DNA-Free RNA Kit (Zymo Research) according to the manufacturer's instructions. RNA quality was assayed using Agilent Technologies 2200 TapeStation and samples with integrity superior to RIN 7 were used for library preparation. Stranded mRNA-Seq libraries were prepared using the Illumina TruSeq Stranded mRNA Library Prep Kit according to the manufacturer's instructions. Briefly, RNA with poly-A tail was isolated using magnetic beads conjugated to poly-T oligos. mRNA was then fragmented and reverse-transcribed into cDNA. dUTPs were incorporated, followed by second strand cDNA synthesis. dUTP-incorporated second strand was not amplified. cDNA was then end-repaired, index adapter-ligated and PCR amplified. AMPure XP beads (Beckman Coulter) were used to purify nucleic acid after each step of the library prep. All sequencing libraries were then quantified, pooled and sequenced at single-end 50 base-pair (bp) on Illumina HiSeq 2500 at the Salk Institute Next Generation Sequencing (NGS) Core. Raw sequencing data were demultiplexed and converted into FASTQ files using CASAVA (v1.8.2).

Sequenced reads were quality-tested using FASTQC (Andrews, 2010; available online at http://www.bioinformatics.babraham.ac.uk/projects/fastqc/) and aligned to the hg19 human genome using the STAR aligner (Dobin et al., 2013) version 2.4.0k. Mapping was carried out using default parameters (up to 10 mismatches per read and up to 9 multi-mapping locations per read). Raw gene expression was quantified across all gene exons (RNA-Seq) using the top-expressed isoform as proxy for gene expression, and differential gene expression was carried out using the edgeR (Robinson et al., 2010) package version 3.6.8 using replicates to compute within-group dispersion. P-values were adjusted to control the false discovery rate (FDR) by the method of Benjamini and Hochberg (Benjamin and Hochberg, 1995). Differentially expressed genes were defined as having a FDR <0.05 and a log2 fold change >1. Hierarchical clustering was performed using the R 3.3.2 software language. The heat map represents the normalized expression of the top expressed genes. Color represents expression from low (white) to high (blue). Principal component analysis was performed using the R 3.3.2 language. Normalized counts were processed using R 3.3.2 software to generate visual graphics for each group. We used DAVID (http://david.abcc.ncifcrf.gov/) to perform the functional GO (Gene Ontology) annotation analyses.

Antibody information

mouse anti-EAAT1 (1:1,000; Santa Cruz, sc-15316)

mouse anti-EAAT2 (1:1,000; Santa Cruz, sc-365634)

rabbit anti-GFAP polyclonal (1:5,000; ThermoFisher Scientific, 01670276)

mouse anti-GAPDH (1:5,000; Fitzgerald Industries International, NC9864008)

mouse anti-nestin (1:500; EMD Millipore, MAB5326MI)

rabbit anti-S100β (1:1,000; Dako, Z031129-2)

mouse anti-GFAP monoclonal (1:250; EMD Millipore, MAB360MI)

rat anti-CD44 (1:100; BD Pharmingen, BDB550538)

rabbit anti-NFIA (1:250; Novus Bio, NBP181406)

mouse anti-ALDH1L1 (1:100; EMD Millipore, MABN495)

mouse IgM anti-A2B5 (1:50; EMD Millipore, MAB312)

donkey anti-mouse HRP (1:5000, GE Healthcare Life Sciences, NA931)

donkey anti-mouse IgG alexa488/cy3/cy5 (1:250, Jackson ImmunoResearch, 715-545-151/ 715-165-151/ 715-175-151)

donkey anti-rabbit HRP (1:5000, GE Healthcare Life Sciences, NA934)

donkey anti-rabbit IgG alexa488/cy3/cy5 (1:250, Jackson ImmunoResearch, 711-545-152/ 711-165-152/ 711-175-152)